ELSEVIER
International Journal of Solids and Structures 41 (2004) 3411–3424
INTERNATIONAL JOURNAL OF SOLIDS and STRUCTURES
www.elsevier.com/locate/ijsolstr

The stability of functionally graded truncated conical shells subjected to aperiodic impulsive loading

A.H. Sofiyev *

Department of Civil Engineering, Suleyman Demirel University, SDU Cunur, 32260 Isparta, Turkey

Received 21 January 2004; received in revised form 21 January 2004
Available online 10 March 2004

Abstract

In this work, the stability of conical shells made of functionally graded materials (FGMs) subject to a uniform external pressure, which is a power function of time, has been studied. The material properties of functionally graded shells are assumed to vary continuously through his thickness of the shell, according to a power law distribution of the volume fractions of the constituents. The fundamental relations, the dynamic stability and compatibility equations of functionally graded truncated conical shells are obtained first. Applying Galerkin's method, these equations have been transformed to a pair of time dependent differential equation with variable coefficient. This differential equation is solved for different initial conditions by variational method by using Lagrange–Hamilton type principle. Thus, general formulas have been obtained for the critical parameters. The results show that the critical parameters are affected by the configurations of the constituent materials, loading parameters variations, the variation of the semi-vertex angle and the power of time in the external pressure expression variations. Comparing results with those in the literature validates the present analysis.

Keywords: Functionally graded materials; Truncated conical shell; Impulsive loading; Critical parameters

1. Introduction

Functionally graded materials (FGMs) are increasingly being considered in various applications to maximize strengths and integrities of many engineering structures. Functionally graded materials have received considerable attention in many engineering applications since they were first reported in 1984 in Japan (see Koizumi, 1993). FGMs are composite materials, microscopically inhomogeneous, in which the mechanical properties vary smoothly and continuously from one surface to the other. This is achieved by gradually varying the volume fraction of the constituent materials. FGMs were initially designed as thermal barrier materials for aerospace structures and fusion reactors. FGMs are now developed for general use as structural components in extremely high temperature environments (see Liew et al., 2002). Investigations of

* Tel.: +90-246-2111243; fax: +90-246-2370859.
E-mail address: asofiyev@mmf.sdu.edu.tr (A.H. Sofiyev).

0020-7683/$ - see front matter
doi:10.1016/j.ijsolstr.2004.02.003

Nomenclature

A_{mn} amplitude
A_β, B_β ($\beta = 1$–6) defined in Eq. (15)
C_{1k}, C_{2k}, C_{3k} $(k = 0, 1, 2)$ defined in Eq. (16)
C_0 integration constant
d power law exponent
E, E_1, E_2 elastic moduli of the materials
e_S, e_θ, $e_{S\theta}$ strain components on the reference surface of the conical shell
F_1, F_2 material property of the constituent's materials
h thickness of the conical shell
i power of time in the external pressure expression
I_{cr} critical stress impulse
j_k $(k = 1, 2)$ coefficient
K_d dynamic factor
M_S, M_θ, $M_{S\theta}$ moment resultants
m wave number in the S direction
N_S, N_θ, $N_{S\theta}$ forces resultants
N_S^0, N_θ^0, $N_{S\theta}^0$ membrane forces in the fundamental configuration
n wave number in the circumferential direction
n_{st}, n_d wave numbers corresponding to the static and dynamic critical loads
$Q_{\alpha\beta}$ reduced stiffness defined in Eqs. (7)–(9)
q_{crs}, q_{crd} static and dynamic critical loads, respectively
q_0, q_1 loading parameter and static external pressure, respectively
$\bar{q}_1$ defined in Eq. (36)
r_1, r_2 average radii of the small and large bases of the conical shell
$S\theta\zeta$ coordinate system on the reference surface of the conical shell
S the axis through the vertex on the reference surface of the cone
S_1, S_2 the inclined distances of the bases of the cone from the vertex
t, t_{cr} time and critical time, respectively
T temperature in Kelvin
V_f volume fractions
w displacement of the reference surface in the inwards normal direction ζ
γ semi-vertex angle of the cone
δ_1, δ_2 defined in Eqs. (35b) and (40), respectively
ν, ν_1, ν_2 Poisson's ratios
τ dimensionless time parameter
ρ, ρ_1, ρ_2 densities of the materials
λ a parameter that depends on the geometry of the conical shell
θ axis lies in the circumferential direction
σ_S, σ_θ, $\sigma_{S\theta}$ stress components
ω defined in Eq. (37)
$\xi_{mn}(t)$, $\eta_{mn}(t)$ time dependent amplitudes
ζ the axis in the inwards normal direction of the reference surface
X defined in Eq. (35a)
Δ_μ $(\mu = -1, 0, 1/2)$ defined in Eq. (31)

Ψ	stress function
Φ_k $(k = 0, 1, 2)$	defined in Eq. (31)
Λ	defined in Eq. (21)
Λ_1, Λ_2	defined in Eqs. (29a) and (29b), respectively
Π	potential energy defined in Eq. (31)

FGM cylindrical shells under different mechanical or thermal loading are limited in number. Studies on FGMs have been extensive but are largely confined to analysis of thermal stress and deformation (see Obata and Noda, 1994; Takezono et al., 1996). Birman (1995) presented a formulation of the stability problem for functionally graded hybrid composite plates, where a micromechanical model was employed to solve the buckling problem for a rectangular plates subjected to uniaxial compression. Feldman and Aboudi (1997) studied elastic bifurcation buckling of FG plates under in-plane compressive loading. In this work the assumed that grades of material properties throughout the structure are produced by a spatial distribution of the local reinforcement volume fraction. Praveen and Reddy (1998) investigated the response of functionally graded ceramic-metal plates using a plate finite element that accounts for the transverse shear strains, rotary inertia and moderately large rotations in the von Karman sense. The static and dynamic response of the functionally graded plates was investigated by varying the volume fraction of the ceramic and metallic constituents using a simple power law distribution. Loy et al. (1999) presented a free vibration analysis of simply supported cylindrical thin shells made of FGM compound of stainless steel and nickel. Reddy (2000) developed theoretical formulations for thick FGM plates according to the higher-order shear deformation plate theory. Then Pradhan et al. (2000) extended this work to the case of FGM cylindrical thin shells under various boundary conditions. Ng et al. (2001) studied the parametric resonance or dynamic stability of FGM cylindrical thin shells under periodic axial loading. In the forgoing studies, Reddy and his co-workers developed a simple theory, in which the material properties are graded in the thickness direction according to a volume fraction power law distribution, but their numerical results were only for the simple case of an FGM shell in a constant thermal environment. Woo and Mequid (2001) gave an analytical solution for large deflection of thin FGM plates and shallow shells. In their studies the thermal load considered arises from the one dimensional steady heat conduction in the plate thickness direction, but the material properties are temperature independent. Pitakthapanaphong and Busso (2002) proposed a self-consistent constitutive framework to describe the behavior of a generic three-layered system containing a functionally graded material (FGM) layer subjected to thermal loading. Shen (2002) presented a post-buckling analysis for a functionally graded cylindrical thin shell of finite length subjected to external pressure and thermal environments. Han et al. (2002) studied transient responses in a functionally graded cylindrical shell to a point load and Zhang et al. (2003) studied transient dynamic analysis of a cracked functionally graded material by a BIEM. Yang and Shen (2003) investigated large deflection and post-buckling responses of functionally graded rectangular plates under transverse and in-plane loads by using a semi-analytical approach.

Thin conical shells composed of different materials have popularity in airspace industry as structural element so; studies on vibration and stability of conical shells are extensive. Many of the studies are for isotropic and composite shells. Among those who have carried out studies on the vibration and stability of conical shells include Mushtari and Sachenkov (1958), Singer (1961, 1966), Tani (1973), Massalas et al. (1981), Irie et al. (1984), Tong et al. (1992), Tong (1993), Babich (1999), and Lam and Hua (1999).

The stability computation of the conical shells under the load that effects for a short time, either depends on dynamic instability criterions and the rule of that load depending on time (form of the impulse). In the solutions of stability problems of conical shells, sometimes obtaining the analytical solutions are impossible due to the difficulties occurring because of the real forms of the influenced loads. According to this, in practice, simple analytical expressions certainly approximate to the real rule of the load change depend on time are used. For example, in some cases effects of the wind and fluid pressure are expressed as the power function of time. There are limited numbers of publications about the stability of thin conical shells under the load depending power function of time. In some of these studies, external pressure is taken into consideration (Shumik, 1973; Sachenkov and Klementev, 1980; Sofiyev and Aksogan, 2002; Sofiyev, 2003). Studies on the stability of conical shells made of FGMs under an external pressure, which is a power function of time, have not been seen in the literature.

In this paper, the stability of functionally graded truncated conical shells subjected to external pressure varying as a power function of time is studied, for different initial conditions by variational method by using Lagrange–Hamilton type principle.

2. Theoretical development

In Fig. 1 is seen a truncated conical shell made of FGM completed to a full cone. The coordinate system is chosen such that the origin O is at the vertex of the whole cone, on the reference surface of the shell, and the S axis lies on the curvilinear reference surface of the cone, the θ axis lies in the circumferential direction on the reference surface of the cone and the ζ axis, being perpendicular to the plane of the first two axes, lies in the inwards normal direction of the cone. The average radii of the small and large bases of the conical shell are r_1 and r_2, and the distances from the vertex to the small and large bases are S_1 and S_2, respectively, and the semi-vertex angle is γ.

In order to accurately model the material properties of functionally graded materials, the properties must be both temperature and position dependent. This is achieved by using a simple rule of mixtures for the stiffness parameters coupled with the temperature dependent properties of the constituents. The volume fraction is a spatial function and the properties of the constituents are functions of the temperature. The combination of these functions gives rise to the effective material properties of functionally graded materials and can be expressed as

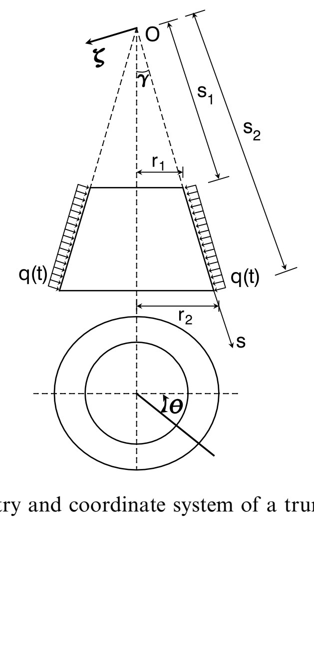

Fig. 1. The geometry and coordinate system of a truncated conical shell.

$$F = F_1 V_{f_1} + F_2 V_{f_2} \tag{1}$$

in which F_1 and F_2 are, respectively the material property of the constituents materials, V_{f_1} and V_{f_2} are the volume fractions of the constituents materials and are related by

$$V_{f_1} + V_{f_2} = 1 \tag{2}$$

We assume the volume fraction follows a simple power law as

$$V_f = (\bar{\zeta} + 0.5)^d, \quad \bar{\zeta} = \zeta/h \tag{3}$$

where volume fraction index $d \geqslant 0$ dictates the material variation profile through the shell thickness and may be varied to obtain the optimum distribution of component materials. It is noted that similar definition may be found in Ng et al. (2001), but is for V_f. From Eqs. (1)–(3), the effective elastic modulus $E(\bar{\xi})$, Poisson's ratio $v(\bar{\xi})$ and density $\rho(\bar{\xi})$ of an FGM shell can be written as

$$\begin{aligned} E(\bar{\xi}) &= (E_1 - E_2)(\bar{\zeta} + 0.5)^d + E_2, \\ v(\bar{\xi}) &= (v_1 - v_2)(\bar{\zeta} + 0.5)^d + v_2, \\ \rho(\bar{\xi}) &= (\rho_1 - \rho_2)(\bar{\zeta} + 0.5)^d + \rho_2 \end{aligned} \tag{4}$$

where E_1, v_1, ρ_1 and E_2, v_2, ρ_2 are the elastic modulus, Poisson's ratio and density of the material 1 and material 2, respectively. From these equations the followings are obtained:

$$\begin{cases} E = E_1, \ v = v_1, \ \rho = \rho_1 & \text{at } \bar{\zeta} = 0.5 \\ E = E_2, \ v = v_2, \ \rho = \rho_2 & \text{at } \bar{\zeta} = -0.5 \end{cases} \tag{5}$$

The material properties vary continuously from material 2 at the inner surface of the conical shell to material 1 at the outer surface of the conical shell.

According to the above distribution described in Eq. (5), the inner surface of the conical shell is ceramic rich and the outer surface is metal rich. We shall name this type A. For a conical shell that is metal rich at the inner surface and ceramic rich at the outer surface, which we shall name Type B.

Therefore, the material properties along the thickness of the shells, such as elastic modulus $E(\bar{\xi})$, Poisson's ratio $v(\bar{\xi})$ can be determined according to Eq. (4). With the help of these material properties, the stress–strain relations for thin conical shells can be determined as,

$$\begin{pmatrix} \sigma_S \\ \sigma_\theta \\ \sigma_{S\theta} \end{pmatrix} = \begin{bmatrix} Q_{11} & Q_{12} & 0 \\ Q_{12} & Q_{22} & 0 \\ 0 & 0 & Q_{66} \end{bmatrix} \begin{pmatrix} e_S - \frac{\partial^2 w}{\partial S^2} \\ e_\theta - \frac{1}{S^2}\frac{\partial^2 w}{\partial \varphi^2} - \frac{1}{S}\frac{\partial w}{\partial S} \\ e_{S\theta} - \frac{1}{S}\frac{\partial^2 w}{\partial S \partial \varphi} + \frac{1}{S^2}\frac{\partial w}{\partial \varphi} \end{pmatrix} \tag{6}$$

where, $\varphi = \theta \sin \gamma$, σ_S, σ_θ and $\sigma_{S\theta}$ are the stresses components, e_S, e_θ and $e_{S\theta}$ are the strains components on the reference surface, w is the displacement of the reference surface in the normal direction, positive towards the axis of the cone and assumed to be much smaller than the thickness and $Q_{\alpha\beta}$ $(\alpha, \beta = 1, 2, 6)$ are defined as:

$$Q_{11} = Q_{22} = \frac{(E_1 - E_2)(\bar{\zeta} + 0.5)^d + E_2}{1 - [(v_1 - v_2)(\bar{\zeta} + 0.5)^d + v_2]^2}, \tag{7}$$

$$Q_{12} = \frac{\left[(E_1 - E_2)\left(\bar{\zeta} + 0.5\right)^d + E_2\right]\left[(v_1 - v_2)(\bar{\zeta} + 0.5)^d + v_2\right]}{1 - [(v_1 - v_2)(\bar{\zeta} + 0.5)^d + v_2]^2}, \tag{8}$$

$$Q_{66} = \frac{(E_1 - E_2)(\bar{\zeta} + 0.5)^d + E_2}{2\left[1 + (v_1 - v_2)\left(\bar{\zeta} + 0.5\right)^d + v_2\right]} \tag{9}$$

It is assumed that a uniform external pressure varying as a power function of time as follows acts the conical shell on:

$$N_S^0 = -0.5 \times S(q_1 + q_0 t^i)\tan\gamma, \quad N_\theta^0 = -S(q_1 + q_0 t^i)\tan\gamma, \quad N_{S\theta}^0 = 0 \tag{10}$$

where N_S^0, N_θ^0, $N_{S\theta}^0$ are the membrane forces in the fundamental configuration, q_0 is the loading parameter, q_1 is the static external pressure, i is a positive whole number power which expresses the time dependence of the external pressure satisfying $i \geqslant 1$ and t is time coordinate.

The force and moment resultants can be calculated using the following expression,

$$(N_S, N_\theta, N_{S\theta}) = h\int_{-0.5}^{0.5}(\sigma_S, \sigma_\theta, \sigma_{S\theta})\,d\bar{\zeta}, \quad (M_S, M_\theta, M_{S\theta}) = h^2\int_{-0.5}^{0.5}(\sigma_S, \sigma_\theta, \sigma_{S\theta})\bar{\zeta}\,d\bar{\zeta} \tag{11}$$

If Airy's stress function Ψ is introduced such that,

$$N_S = \frac{1}{S^2}\frac{\partial^2\Psi}{\partial\varphi^2} + \frac{1}{S}\frac{\partial\Psi}{\partial S}, \quad N_\theta = \frac{\partial^2\Psi}{\partial S^2}, \quad N_{S\theta} = -\frac{1}{S}\frac{\partial^2\Psi}{\partial S\partial\varphi} + \frac{1}{S^2}\frac{\partial\Psi}{\partial\varphi} \tag{12}$$

then the dynamic stability and compatibility equations can be reduced to

$$\begin{aligned} L_1(\Psi, w) \equiv{}& A_2\frac{\partial^4\Psi}{\partial S^4} + \frac{2A_2}{S}\frac{\partial^3\Psi}{\partial S^3} + \frac{S\cot\gamma - A_2}{S^2}\frac{\partial^2\Psi}{\partial S^2} + \frac{A_2}{S^3}\frac{\partial\Psi}{\partial S} + \frac{A_2}{S^4}\frac{\partial^4\Psi}{\partial\varphi^4} \\ &+ \frac{2(A_1 - A_5)}{S^2}\frac{\partial^4\Psi}{\partial S^2\partial\varphi^2} + \frac{2(A_5 - A_1)}{S^3}\frac{\partial^3\Psi}{\partial S\partial\varphi^2} + \frac{2(A_1 - A_5 + A_2)}{S^4}\frac{\partial^2\Psi}{\partial\varphi^2} - \frac{A_3}{S^4}\frac{\partial^4 w}{\partial\varphi^4} \\ &- \frac{2(A_4 + A_6)}{S^2}\frac{\partial^4 w}{\partial S^2\partial\varphi^2} + \frac{2(A_4 + A_6)}{S^3}\frac{\partial^3 w}{\partial S\partial\varphi^2} - \left[\frac{q_1 + q_0 t^i}{S\cot\gamma} + \frac{2(A_4 + A_6 + A_3)}{S^4}\right]\frac{\partial^2 w}{\partial\varphi^2} - A_3\frac{\partial^4 w}{\partial S^4} \\ &- \frac{2A_3}{S}\frac{\partial^3 w}{\partial S^3} + \left(\frac{A_3}{S^2} - \frac{(q_1 + q_0 t^i)S}{2\cot\gamma}\right)\frac{\partial^2 w}{\partial S^2} - \left(\frac{q_1 + q_0 t^i}{\cot\gamma} + \frac{A_3}{S^3}\right)\frac{\partial w}{\partial S} - \rho_t h\frac{\partial^2 w}{\partial t^2} \\ &= 0 \end{aligned} \tag{13}$$

$$\begin{aligned} L_2(\Psi, w) \equiv{}& \frac{B_1}{S^4}\frac{\partial^4\Psi}{\partial\varphi^4} + \frac{2(B_5 + B_2)}{S^2}\frac{\partial^4\Psi}{\partial S^2\partial\varphi^2} - \frac{2(B_5 + B_2)}{S^3}\frac{\partial^3\Psi}{\partial S\partial\varphi^2} + \frac{2(B_5 + B_2 + B_1)}{S^4}\frac{\partial^2\Psi}{\partial\varphi^2} + \frac{B_1}{S^3}\frac{\partial\Psi}{\partial S} \\ &+ \frac{B_2 - B_1}{S^2}\frac{\partial^2\Psi}{\partial S^2} + \frac{2B_1}{S}\frac{\partial^3\Psi}{\partial S^3} + B_1\frac{\partial^4\Psi}{\partial S^4} - \frac{B_4}{S^4}\frac{\partial^4 w}{\partial\varphi^4} - \frac{2(B_6 - B_3)}{S^2}\frac{\partial^4 w}{\partial S^2\partial\varphi^2} + \frac{2(B_6 - B_3)}{S^3}\frac{\partial^3 w}{\partial S\partial\varphi^2} \\ &+ \frac{2(B_6 - B_3 - B_4)}{S^4}\frac{\partial^2 w}{\partial\varphi^2} - \frac{B_4}{S^3}\frac{\partial w}{\partial S} + \left(\frac{B_4}{S^2} + \frac{\cot\gamma}{S}\right)\frac{\partial^2 w}{\partial S^2} - \frac{2B_4}{S}\frac{\partial^3 w}{\partial S^3} - B_4\frac{\partial^4 w}{\partial S^4} \\ &= 0 \end{aligned} \tag{14}$$

in which expressions A_β, B_β $(j = 1\text{–}6)$ and ρ_t are defined as follows:

$$A_1 = C_{11}B_1 + C_{21}B_2, \quad A_2 = C_{11}B_2 + C_{21}B_1, \quad A_3 = C_{11}B_3 + C_{21}B_4 + C_{12},$$
$$A_4 = C_{11}B_4 + C_{21}B_3 + C_{22}, \quad A_5 = C_{61}B_5, \quad A_6 = C_{61}B_6 + C_{62}, \quad B_1 = C_{10}D,$$
$$B_2 = -C_{20}D, \quad B_3 = (C_{20}C_{21} - C_{11}C_{10})D, \quad B_4 = (C_{20}C_{11} - C_{21}C_{10})D, \quad B_5 = 1/C_{60},$$
$$B_6 = C_{61}/C_{60}, \quad D = 1/[(C_{10})^2 - (C_{20})^2], \quad \rho_t = \int_{-0.5}^{0.5} [(\rho_1 - \rho_2)(\bar{\zeta} + 0.5)^d + \rho_2]\,\mathrm{d}\bar{\zeta} \tag{15}$$

in which expressions C_{1k}, C_{2k} and $C_{6k}(k = 0, 1, 2)$ are defined as follows:

$$C_{1k} = h^{k+1}\int_{-0.5}^{0.5} \bar{\zeta}^k \frac{(E_1 - E_2)(\bar{\zeta} + 0.5)^d + E_2}{1 - [(v_1 - v_2)(\bar{\zeta} + 0.5)^d + v_2]^2}\,\mathrm{d}\bar{\zeta}, \tag{16a}$$

$$C_{2k} = h^{k+1}\int_{-0.5}^{0.5} \bar{\zeta}^k \frac{[(E_1 - E_2)(\bar{\zeta} + 0.5)^d + E_2][(v_1 - v_2)(\bar{\zeta} + 0.5)^d + v_2]}{1 - [(v_1 - v_2)(\bar{\zeta} + 0.5)^d + v_2]^2}\,\mathrm{d}\bar{\zeta}, \tag{16b}$$

$$C_{6k} = h^{k+1}\int_{-0.5}^{0.5} \bar{\zeta}^k \frac{(E_1 - E_2)(\bar{\zeta} + 0.5)^d + E_2}{1 + (v_1 - v_2)(\bar{\zeta} + 0.5)^d + v_2}\,\mathrm{d}\bar{\zeta} \tag{16c}$$

3. Solution of the problem

Since the conical shell is considered to be simply supported along the peripheries of both bases, the displacement and stress functions, w and Ψ, can be chosen as follows:

$$w = \sum_m \sum_n \xi_{mn}(t)\mathrm{e}^{\lambda r} \sin m_1 r \cos n_1 \varphi \tag{17}$$

$$\Psi = \sum_m \sum_n \eta_{mn}(t) S_2 \mathrm{e}^{(\lambda+1)r} \sin m_1 r \cos n_1 \varphi \tag{18}$$

where $m_1 = m\pi/\ln(S_2/S_1)$, $r = \ln(S/S_2)$, $n_1 = n/\sin\gamma$, $\xi_{mn}(t)$ and $\eta_{mn}(t)$ are variations of time dependent amplitudes, m is the wave number in the S direction, n is the wave number in the circumferential direction, λ is the parameter dependent on the geometry of the conical shell and $1.2 \leqslant \lambda \leqslant 2.0$ (see Sofiyev, 2003).

After applying $r = \ln(S/S_2)$ transformation to system of equations (13) and (14) and applying Galerkin method the following equations obtained as

$$\begin{aligned} &\int_0^{2\pi\sin\gamma}\int_{-\ln(S_2/S_1)}^{0} L_1(\Psi, w) w S_2^2 \mathrm{e}^{2r}\,\mathrm{d}r\,\mathrm{d}\varphi = 0 \\ &\int_0^{2\pi\sin\gamma}\int_{-\ln(S_2/S_1)}^{0} L_2(\Psi, w) \Psi S_2^2 \mathrm{e}^{2r}\,\mathrm{d}r\,\mathrm{d}\varphi = 0 \end{aligned} \tag{19}$$

The equations obtained after writing expressions (17) and (18) in the system of equation (19) and integration, by taking derivatives with respect to variables φ and S, each at a time, it is noted that, the functions involved in them should be steeply increasing with respect to φ and varying slowly with respect to S. For $m = 1$, taking above properties and the terms $\xi_{mn}(t)$ and $\eta_{mn}(t)$ from the series into consideration, neglecting small terms and eliminating $\eta_{mn}(t)$ from the equations, thus obtained, one gets

$$\frac{\mathrm{d}^2\xi_{mn}(\tau)}{\mathrm{d}\tau^2} + \Lambda(\tau)\xi_{mn}(\tau) = 0 \tag{20}$$

in which $t = t_{cr}\tau$, t_{cr} being the critical time and τ being the dimensionless time parameter such that $0 \leqslant \tau \leqslant 1$. In Eq. (20) the following definitions apply:

$$\Lambda(\tau) = \frac{t_{cr}^2}{\rho_t h S_2^2}\left[\left(A_3 - \frac{A_2 B_4}{B_1}\right)\frac{\Delta_{-1} n_1^4}{S_2^2} + \frac{m_2^2}{n_1^4}\frac{\Delta_0}{B_1}\cot^2\gamma - n_1^2 \Delta_{1/2}(q_1 + q_0 t_{cr}^i \tau^i) S_2 \tan\gamma\right] \tag{21}$$

$$m_2^2 = (m_1^2 + \lambda^2)(m_1^2 + \lambda^2 - 1) \tag{22}$$

$$\Delta_\mu = \frac{[1 - (S_1 S_2^{-1})^{2(\lambda+\mu)}][m_2^2 + (\lambda+1)^2](\lambda+1)}{[1 - (S_1 S_2^{-1})^{2(\lambda+1)}][m_2^2 + (\lambda+\mu)^2](\lambda+\mu)}, \quad \mu = -1, 0, 1/2 \tag{23}$$

The solution of this problem is transformed to the solution of second order differential equation with variable coefficient dependent on time that satisfies the initial condition as in the following:

$$\xi = 0, \quad \frac{\partial \xi}{\partial \tau} = 0 \quad \text{when } \tau = 0 \tag{24}$$

Because of (ξ, τ) curve has a maximum at $\tau = 1$ the initial condition is taken up as,

$$\xi = 0 \quad \text{when } \tau = 0 \quad \text{and} \quad \frac{\partial \xi(1)}{\partial \tau} = 0 \quad \text{when } \tau = 1 \tag{25}$$

Eq. (20) is solved by variational method by using Lagrange–Hamilton type principle. The approximating functions satisfying (24) and (25) has been chosen as a first approximation in the following form:

$$\xi_{mn}(\tau) = A_{mn}\xi(\tau) = A_{mn} e^{j_1 \tau} \tau^2 [(j_1 + 3)(j_1 + 2)^{-1} - \tau] \tag{26}$$

$$\xi_{mn}(\tau) = A_{mn}\xi(\tau) = A_{mn} e^{j_2 \tau} \tau [(j_2 + 2)(j_2 + 1)^{-1} - \tau] \tag{27}$$

The minimum value of critical load is dependent on selection of the function $\xi(\tau)$ so, it is dependent on the values of j_k $(k = 1, 2)$ coefficient. It is determined numerically that after the computations, lest one of the minimum values of critical load corresponds to $j_k = i + 1$ $(k = 1, 2)$. Here, A_{mn} is the unknown displacement amplitude.

Multiplying Eq. (20) by $\xi'_\tau(\tau)$ then after integration, the following equation is obtained:

$$\left[\frac{d\xi(\tau)}{d\tau}\right]^2 + \Lambda_1[\xi(\tau)]^2 - 2\Lambda_2 \int \xi(\tau)\frac{d\xi(\tau)}{d\tau}\tau^i \, d\tau = C_0 \tag{28}$$

where C_0 is integration constant and it is assumed that the initial conditions that taken up into consideration is equal to zero. Besides, in any points of interval $0 < \tau < 1$, $\xi'_\tau(\tau)$ is not equal to zero and the following definitions apply:

$$\Lambda_1 = \frac{t_{cr}^2}{\rho_t h S_2^2}\left[\left(A_3 - \frac{A_2 B_4}{B_1}\right)\frac{\Delta_{-1}}{S_2^2} n_1^4 + \frac{m_2^2}{n_1^4}\frac{\Delta_0}{B_1}\cot^2\gamma - q_1 n_1^2 \Delta_{1/2} S_2 \tan\gamma\right] \tag{29a}$$

$$\Lambda_2 = \frac{q_0 n_1^2 t_{cr}^{2+i} \Delta_{1/2} \tan\gamma}{\rho_t h S_2} \tag{29b}$$

Substituting Eqs. (26) and (27) in (28), then after integration in $0 \leqslant \tau \leqslant 1$, for Lagrange–Hamilton type functional the following expression is obtained:

$$\Pi = A_{mn}\left\{\frac{\Phi_1 \rho_t h S_2^4}{t_{cr}^2 n_1^2 \tan\gamma} - \Phi_2 q_0 t_{cr}^i S_2^3 \Delta_{1/2} + \Phi_0\left[\left(A_3 - \frac{A_2 B_4}{B_1}\right)\frac{\Delta_{-1}}{\tan\gamma} n_1^2 + \frac{S_2^2 m_2^2 \Delta_0}{B_1 \tan^3\gamma}\frac{1}{n_1^6} - q_1 \Delta_{1/2} S_2^3\right]\right\} \tag{30}$$

Table 1
The values of $\Phi_k,\ k = 0, 1, 2$ for different values power of time i

	$i = 1$	$i = 2$	$i = 3$	$i = 4$
$\xi(\tau) = e^{j_1\tau}\tau^2[(j_1+3)(j_1+2)^{-1} - \tau]$				
Φ_0	0.8859	3.5645	15.809	75.2705
Φ_1	4.6561	24.700	142.836	870.4636
Φ_2	0.5789	1.8139	6.8670	29.3800
$\xi(\tau) = e^{j_2\tau}\tau[(j_2+2)(j_2+1)^{-1} - \tau]$				
Φ_0	2.086	7.0527	27.7911	121.533
Φ_1	6.678	30.8768	168.032	992.333
Φ_2	1.1430	2.9326	9.9737	39.916

where

$$\Phi_0 = \int_0^1 [\xi(\tau)]^2 \, d\tau, \quad \Phi_1 = \int_0^1 [\xi'_\tau(\tau)]^2 \, d\tau, \quad \Phi_2 = 2\int_0^1\int_0^\tau \eta^i \xi'_\tau(\eta)\xi(\eta) \, d\eta \, d\tau \tag{31}$$

The values of the Φ_k, $k = 0, 1, 2$ given in Table 1.

During in finite time, there may be no agreement in the work done by external forces and inertia force and the minimum value of potential energy. According to this, being the minimum condition in respect of unknown amplitude A_{mn} of the functional Π, must supported by being the minimum condition in respect of n_1^2 wave number of the functional Π. These two conditions gives the following two algebraically equations dependent on t_{cr} and n_1:

$$\frac{\partial \Pi}{\partial A_{mn}} = \frac{\Phi_1 \rho_t h S_2^4}{t_{cr}^2 \tan\gamma} \frac{1}{n_1^2} - \Phi_2 q_0 t_{cr}^i S_2^3 \Delta_{1/2} + \Phi_0 \left[\left(A_3 - \frac{A_2 B_4}{B_1} \right) \frac{\Delta_{-1}}{\tan\gamma} n_1^2 + \frac{S_2^2 m_2^2 \Delta_0}{B_1 \tan^3\gamma} \frac{1}{n_1^6} - q_1 \Delta_{1/2} S_2^3 \right] = 0 \tag{32}$$

$$\frac{\partial \Pi}{\partial n_1^2} = \Phi_0 \left[\left(A_3 - \frac{A_2 B_4}{B_1} \right) \frac{\Delta_{-1}}{\tan\gamma} - \frac{3 S_2^2 m_2^2 \Delta_0}{B_1 \tan^3\gamma} \frac{1}{n_1^8} \right] - \frac{\Phi_1 \rho_t h S_2^4}{t_{cr}^2 \tan\gamma} \frac{1}{n_1^4} = 0 \tag{33}$$

Eliminating t_{cr} from Eqs. (32) and (33), the following equation is obtained:

$$(1 - 3X)^{i/2}(1 - X - 0.5\bar{q}_1 X^{1/4}) = q_0 \omega^{i/2} X^{(1+i)/4} \tag{34}$$

where the following definitions apply:

$$X = \delta_1 \frac{\cot^2\gamma}{n_1^8}, \tag{35a}$$

$$\delta_1 = \frac{m_2^2 S_2^2}{(A_3 B_1 - A_2 B_4)} \frac{\Delta_0}{\Delta_{-1}}, \tag{35b}$$

$$\bar{q}_1 = \frac{\Delta_{1/2} S_2^{5/2} B_1^{1/4} q_1}{\Delta_0^{1/4} [(A_3 B_1 - A_2 B_4)\Delta_{-1}]^{3/4} \cot^{3/2}\gamma}, \tag{36}$$

$$\omega = \frac{\Phi_1 \Phi_2^{2/i} \rho_t h (\Delta_{1/2})^{2/i} S_2^{(3i+5)/i} B_1^{(2+i)/i}}{2^{2/i} \Phi_0^{(2+i)/i} [m_2^2 \Delta_0]^{(1+i)/(2i)} [(A_3 B_1 - A_2 B_4)\Delta_{-1} \cot^2\gamma]^{(3+i)/(2i)}} \tag{37}$$

For $q_1 = 0$ and large values of the loading parameters, solving Eq. (34) for X and by putting this expression in (35) and taking the relation $n_1 = n/\sin\gamma$ into consideration, the following expression is obtained:

$$n_{\mathrm{d}}^2 = \frac{1}{\sqrt{2}}\delta_1^{1/4} q_0^{1/(1+i)} \omega^{i/(2+2i)} \sin^{1/2}(2\gamma)\sin\gamma \tag{38}$$

where the wave number n_{d}, which is dependent on the way the dynamic load varies, characterizes the form of loss of stability of the shell under the dynamic load.

Substituting expression (38) in Eq. (32), the dynamic critical load is found as follows:

$$q_{\mathrm{crd}} = q_0 t_{\mathrm{cr}}^i = \frac{2\delta_2 \Phi_0}{\Phi_2} q_0^{1/(1+i)} \omega^{i/(2+2i)} \tag{39}$$

where

$$\delta_2 = \frac{\Delta_0^{1/4}}{\Delta_{1/2}} \frac{m_2^{1/2} \Delta_{-1}^{3/4} (A_3 B_1 - A_2 B_4)^{3/4}}{B_1 S_2^{5/2}} \cot^{3/2}\gamma \tag{40}$$

In the static case ($t_{\mathrm{cr}} \to \infty,\ q_0 \to 0$), from Eq. (33) the following equation is found for the wave number corresponding to the static critical load:

$$n_{\mathrm{st}}^2 = 0.75^{0.25} \delta_1^{1/4} \sin^{1/2}(2\gamma)\sin\gamma \tag{41}$$

Substituting expression (41) in Eq. (32) and replacing $q_0 t_{\mathrm{cr}}^i / \Phi_0$, the static critical load is found as

$$q_{\mathrm{crs}} = \frac{4\delta_2}{3^{3/4}} \tag{42}$$

and, from the definition $K_{\mathrm{d}} = q_{\mathrm{crd}}/q_{\mathrm{crs}}$, the dynamic factor is given as

$$K_{\mathrm{d}} = \frac{3^{3/4}\Phi_0}{2\Phi_2} q_0^{1/(1+i)} \omega^{i/(2+2i)} \tag{43}$$

The critical time and critical stress impulse can be found

$$t_{\mathrm{cr}} = \left(\frac{2\delta_2 \Phi_0}{\Phi_2}\right)^{1/i} q_0^{1/(1+i)} \omega^{1/(2+2i)} \tag{44}$$

$$I_{\mathrm{cr}} = \int_0^{t_{\mathrm{cr}}} q_0 t^i \,\mathrm{d}t = \left[\frac{2\Phi_0 \delta_2}{\Phi_2}\right]^{(1+i)/i} \frac{\omega^{1/2}}{1+i} \tag{45}$$

4. Numerical computations and results

The ceramic material used in this study is silicon nitride and the metal material used is nickel. The densities and Poisson's ratios of the materials are in this case independent of the temperature. The density of silicon nitride is taken to be 2370 (kg/m^3) and that of nickel 8900 (kg/m^3). The Poisson's ratio is 0.24 for silicon nitride and 0.31 for nickel. The elastic moduli are however, temperature dependent and are obtained from Ng et al. (2001) and Touloukian (1967) as

$$E_{\mathrm{sn}} = 348.43 \times 10^9 (1 - 3.070 \times 10^{-4} T + 2.160 \times 10^{-7} T^2 - 8.946 \times 10^{-11} T^3) \tag{46}$$

$$E_{\mathrm{ni}} = 223.95 \times 10^9 (1 - 2.794 \times 10^{-4} T - 3.998 \times 10^{-9} T^2) \tag{47}$$

where E_{sn} and E_{ni} are the elastic moduli (in Pa) of silicon nitride and nickel, respectively, and $T = 300$ K is the temperature in Kelvin.

Table 2
Variation of the critical parameters with semi-vertex angle γ for $q_0 = 225$ (MPa/s) ($\xi(0) = 0$, $\xi'_\tau(1) = 0$, $\xi(\tau) = e^{2\tau}\tau[3/2 - \tau]$)

γ	$d^{SN} = 0$	Type A material					$d^{N} = 0$
		$d = 0.5$	$d = 1$	$d = 2$	$d = 3$	$d = 4$	
q_{crd} (MPa)							
30°	0.0791	0.0768	0.0744	0.07123	0.0694	0.0682	0.0629
45°	0.0715	0.0694	0.0672	0.06437	0.0627	0.0616	0.0569
60°	0.0601	0.0583	0.0565	0.05413	0.0527	0.0518	0.0478
$I_{cr} \times 10^5$ (MPa s)							
30°	13.895	13.107	12.2981	11.276	10.698	10.334	8.0803
45°	11.346	10.702	10.0413	9.2069	8.7350	8.4377	7.1875
60°	8.0224	7.5674	7.10030	6.5102	6.1766	5.9663	5.0823
K_d							
30°	3.0458	2.5047	2.2937	2.0920	1.9871	1.9204	1.5919
45°	2.6378	2.1692	1.9864	1.8117	1.7209	1.6631	1.3786
60°	3.0458	2.5047	2.2937	2.0920	1.9871	1.9204	1.5919

Table 3
Variation of the critical parameters with semi-vertex angle γ for $q_0 = 225$ (MPa/s) ($\xi(0) = 0$, $\xi'_\tau(1) = 0$, $\xi(\tau) = e^{2\tau}\tau[3/2 - \tau]$)

γ	$d^{SN} = 0$	Type B material					$d^{N} = 0$
		$d = 0.5$	$d = 1$	$d = 2$	$d = 3$	$d = 4$	
q_{crd} (MPa)							
30°	0.0791	0.0715	0.0744	0.0769	0.0781	0.0787	0.0629
45°	0.0715	0.0646	0.0672	0.0695	0.0705	0.0711	0.0569
60°	0.0601	0.0544	0.0565	0.0584	0.0593	0.0598	0.0478
$I_{cr} \times 10^5$ (MPa s)							
30°	13.895	11.368	12.298	13.145	13.537	13.749	8.0803
45°	11.346	9.2817	10.141	10.733	11.053	11.226	7.1875
60°	8.0224	6.5632	7.1003	7.5894	7.8158	7.9378	5.0823
K_d							
30°	3.0458	2.0752	2.2937	2.4973	2.5971	2.6597	1.5919
45°	2.6378	1.7972	1.9864	2.1627	2.2492	2.3034	1.3786
60°	3.0458	2.0752	2.2937	2.4973	2.5971	2.6598	1.5919

The stability results for the FGM conical shell presented in Tables 2 and 3 are for simply supported silicon nitride–nickel FGM conical shell of geometric properties $r_1 = 2.25 \times 10^{-2}$ (m), $r_2 = 8 \times 10^{-2}$ (m), $h = 1.3 \times 10^{-4}$ (m), $\lambda = 1.2$ for both Type A and Type B materials. Results presented are for different values of the power law exponent d and different loading parameters. Type A material, when $d = 0$, the shell is fully ceramic (silicon nitride) and Type B material, when $d = 0$, the shell is fully metal (nickel).

Comparing the dynamic critical load, critical impulse and dynamic factor values in Table 2 with those in Table 3, it can be seen that for power law exponent $d > 1$, the critical parameters values for a Type B material are higher than a Type A material. For power law exponent $d = 1$, critical parameters values for Type A and B materials are equal. On the other hand, for power law exponent $d < 1$ the critical parameters values for a Type A material are higher than a Type B material. For example, for power law exponent $d = 4$ the dynamic critical load, critical impulse and dynamic factor for a Type B material is about 13.5%, 24.84% and 27.8% higher than a Type A material, respectively. When the coefficient d increases, the percentages increase a little. For the power law exponent $d = 0.5$, the dynamic critical load, critical impulse and

Table 4
The variation of the critical parameters with both forms of $\xi(\tau)$ and power of time i for $\gamma = 75°$

	$i = 1$, $q_0 = 2.25 \times 10^2$ MPa/s			$i = 2$, $q_0 = 5 \times 10^4$ MPa/s^2			$i = 3$, $q_0 = 5 \times 10^7$ MPa/s^3		
	$d = 0.5$	$d = 1$	$d = 2$	$d = 0.5$	$d = 1$	$d = 2$	$d = 0.5$	$d = 1$	$d = 2$
$\xi(0) = 0$, $\xi'_\tau(1) = 0$, $\xi(\tau) = e^{2\tau}\tau[3/2 - \tau]$									
Type A material									
q_{crd} (MPa)	0.0420	0.041	0.039	0.0194	0.0186	0.0175	0.0217	0.021	0.0194
K_d	4.3383	3.973	3.623	2.0034	1.8153	1.6319	2.242	2.022	1.8045
$I_{cr} \times 10^7$ (MPa s)	391.71	367.5	336.9	0.380	0.3400	0.3800	0.0047	0.0042	0.0038
Type B material									
q_{crd} (MPa)	0.039	0.041	0.042	0.018	0.019	0.0194	0.020	0.021	0.022
K_d	3.594	3.973	4.326	1.621	1.815	1.999	1.794	2.022	2.238
$I_{cr} \times 10^7$ (MPa s)	339.7	367.5	392.9	0.311	0.345	0.377	0.0038	0.0043	0.0047
$\xi(0) = 0$, $\xi'_\tau(0) = 0$, $\xi(\tau) = e^{2\tau}\tau^2[4/3 - \tau]$									
Type A material									
q_{crd} (MPa)	0.043	0.042	0.040	0.0198	0.0189	0.0179	0.0219	0.0209	0.020
K_d	4.497	4.118	3.756	2.0406	1.849	1.662	2.260	2.037	1.818
$I_{cr} \times 10^7$ (MPa s)	420.9	394.9	362.1	0.3900	0.3583	0.319	0.0048	0.0044	0.0038
Type B material									
q_{crd} (MPa)	0.0436	0.042	0.044	0.018	0.019	0.0197	0.020	0.021	0.022
K_d	4.484	4.118	4.484	1.651	1.849	2.036	1.807	2.037	2.255
$I_{cr} \times 10^7$ (MPa s)	422.1	394.9	422.2	0.323	0.358	0.392	0.0039	0.004	0.005

dynamic factor for a Type A material is about 7.4%, 15.3% and 20.7% higher than a Type B material, respectively. For all power law exponent d the dynamic critical load, critical impulse and dynamic factor fall between those for d^{SN} and d^{N}. It is observed that the effect of volume fractions and the configurations of the constituent materials on dynamic factor are more important. As the semi-vertex angle γ increases, the values of the dynamic critical load and critical impulse decrease, whereas the values of the dynamic factor decrease for $\gamma \leqslant 45°$ and increase for $\gamma > 45°$. Variations of the elastic moduli resulting from another values of γ do not change the behavior of the critical parameters.

The variation of the dynamic critical load, critical impulse and dynamic factor of Type A and Type B materials with different approximation function and the power of time i are presented in Table 4. The numerical analysis for the conical shell parameters which are taken into consideration show that the loading parameter varies approximately by the following values to become the loading dynamic: (a) when $N_\theta^0 = -q_0 t S \tan\gamma$ or $i = 1$, namely the external pressure varies linearly depending on time, it must be in $0.8439 \leqslant \hat{q} < 4.219$, (b) when $N_\theta^0 = -q_0 t^2 S \tan\gamma$ or $i = 2$, namely the external pressure varies parabolic depending on time, it must be in $4.219 \leqslant \hat{q} < 8.439 \times 10^2$, (c) when $N_\theta^0 = -q_0 t^3 S \tan\gamma$ or $i = 3$, namely the external pressure varies cubically depending on time, it must be in $8.439 \times 10^2 \leqslant \hat{q} \leqslant 4.219 \times 10^5$. Here, $\hat{q} = q_0 R_1 / E_1 h$ definition is valid. Consequently when the loading law changes, the values of loading parameter changes, too. It is indicated from Table 4, for both forms of $\xi(\tau)$ approximation functions, the maximum difference between the critical parameter values is about 3%. Furthermore, both of approximation functions can be used in the same way. Besides, difference between values of the dynamic factors, dynamic critical load and critical impulse of Type A and Type B materials increases, when i increases, for

Table 5
Comparison of critical parameters

γ	Experimentally (Sachenkov and Klementev, 1980)		Numerically (Shumik, 1973)		Present study	
	q_{crd} (MPa)	K_d	q_{crd} (MPa)	K_d	q_{crd} (MPa)	K_d
20°	0.0575	2.880	0.0767	3.8788	0.0796	4.0259
30°	0.0726	2.690	0.0736	2.8790	0.0764	2.9882
40°	0.0810	2.700	0.0693	2.5317	0.0719	2.6277

power law exponent $d > 1$. When the loading form changes and the power of time i increase, the critical impulse values decrease in an important degree.

To validate the analysis, results for simply supported conical shells are compared in Table 5 with Shumik (1973) that was solved numerically by using energy method, Lagrange equation and Runge–Kutta method and with Sachenkov and Klementev (1980) that was solved experimentally. The comparisons with those methods were carried out for the following isotropic material, shell and loading properties:

$$E = 2.11 \times 10^5 \ (\text{MPa}), \quad \nu = 0.3, \quad \rho = 8 \times 10^3 \ (\text{kg/m}^3), \quad h = 1.3 \times 10^{-4} \ (\text{m}),$$
$$r_1 = 2.25 \times 10^{-2} \ (\text{m}), \quad r_2 = 8 \times 10^{-2} \ (\text{m}), \quad i = 1, \quad q_0 = 225 \ (\text{MPa/s}), \quad \lambda = 1.2, \quad \gamma = 40°.$$

5. Conclusions

The stability of truncated conical shells of functionally graded material subjected to external pressure varying as a power function of time was investigated. Taking the large values of loading parameters into consideration, analytic solutions are obtained for different initial conditions for critical parameters values. Results were found to vary significantly when material distribution was varied by changing the values of the power law exponent, which controls the volume fraction of the different materials in the FGM shell. It was also found that reasonable control could be achieved on the critical parameters values by correctly varying the power law exponent. A validation of the analysis has been carried out by comparing results with those in the literature and has found to be accurate.

References

Babich, D.V., 1999. Natural vibrations of a conical orthotropic shell with small curvatures of the generatrix. Int. Appl. Mech. 35, 276–280.

Birman, V., 1995. Buckling of functionally graded hybrid composite plates. In: Proc. 10th Conf. Engng. Mech., Boulder, USA.

Feldman, E., Aboudi, J., 1997. Buckling analysis of functionally graded plates subjected to uniaxial loading. Compos. Struct. 38, 29–36.

Han, X., Xu, D., Liu, G.R., 2002. Transient responses in a functionally graded cylindrical shell to a point load. J. Sound Vibr. 25, 783–805.

Irie, T., Yamada, G., Kaneko, Y., 1984. Natural frequencies of truncated conical shells. J. Sound Vibr. 92, 447–453.

Koizumi, M., 1993. The concept of FGM. Ceram. Trans. Function. Grad. Mater. 34, 3–10.

Lam, K.Y., Hua, L., 1999. Influence of boundary conditions on the frequency characteristics of a rotating truncated circular conical shell. J. Sound Vibr. 223, 171–195.

Liew, K.M., He, X.Q., Ng, T.Y., Kitipornchai, S., 2002. Active control of FGM shell subjected to a temperature gradient via piezoelectric sensor/actuator patches. Int. J. Numer. Meth. Engng. 55, 653–668.

Loy, C.T., Lam, K.Y., Reddy, J.N, 1999. Vibration of functionally graded cylindrical shells. Int. J. Mech. Sci. 1, 309–324.

Massalas, C., Dalamanagas, D., Tzivanidis, G., 1981. Dynamic instability of truncated conical shells with variable modulus of elasticity under periodic compressive forces. J. Sound Vibr. 79, 519–528.
Mushtari, K.M., Sachenkov, A.V., 1958. Stability of cylindrical and conical shells of circular cross section with simultaneous action of axial compression and external normal pressure, NASA TM-1433.
Ng, T.Y., Lam, K.Y., Liew, K.M., Reddy, N.J., 2001. Dynamic stability analysis of functionally graded cylindrical shells under periodic axial loading. Int. J. Solids Struct. 38, 1295–1309.
Obata, Y., Noda, N., 1994. Steady thermal stress in a hollow circular cylinder and a hollow sphere of a functionally gradient material. J. Thermal Stress. 17, 471–487.
Pitakthapanaphong, S., Busso, E.P., 2002. Self-consistent elasto-plastic stress solutions for functionally graded material systems subjected to thermal transients. J. Mech. Phys. Solids 50, 695–716.
Pradhan, S., Loy, C., Lam, K.Y., Reddy, J.N., 2000. Vibration characteristics of functionally graded cylindrical shells under various boundary conditions. Appl. Acoust. 61, 11–129.
Praveen, G.V., Reddy, J.N., 1998. Nonlinear transient thermo-elastic analysis of functionally graded ceramic-metal plates. Int. J. Solids Struct. 35, 4457–4476.
Reddy, J.N., 2000. Analysis of functionally graded plates. Int. J. Numer. Meth. Engng. 47, 663–684.
Sachenkov, A.V., Klementev, G.G., 1980. Research of the stability of conical shells by theoretical–experimental method under impulsive load. Research on the Theory of Plates and Shells, Kazan State University, Kazan, 15, pp. 115–125 (in Russian).
Shen, H.S., 2002. Postbuckling analysis of pressure-loaded functionally graded cylindrical shells in thermal environments. Compos. Sci. Technol. 62, 977–987.
Shumik, M.A., 1973. The stability of a truncated conical shell subject to a dynamic external pressure (in Russian). Soviet Appl. Mech. 9, 107–109.
Singer, J., 1961. Buckling of circular conical shells under axi-symmetrical external pressure. J. Mech. Engng. Sci. 3, 330–339.
Singer, J., 1966. Buckling of damped conical shells under external pressure. AIAA J. 4, 328–337.
Sofiyev, A.H., 2003. The buckling of an orthotropic composite truncated conical shell with continuously varying thickness subject to a time dependent external pressure. Compos. Part B—Engng. 34, 227–233.
Sofiyev, A.H., Aksogan, O., 2002. The dynamic stability of a non-homogeneous orthotropic elastic conical shell under a time dependent external pressure. Struct. Engng. Mech. 13, 329–343.
Takezono, S., Tao, K., Inamura, E., Inoue, M., 1996. Thermal stress and deformation in functionally graded material shells of revolution under thermal loading due to fluid. JSME Int. J. Series A: Mech. Mater. Engng. 39, 573–581.
Tani, J., 1973. Dynamic stability of truncated conical shells under periodic external pressure. The Report of the Institute of High Speed Mechanics, Tohoku University, Japan, 28, pp. 135–147.
Tong, L., 1993. Free vibration of orthotropic conical shells. Int. J. Engng. Sci. 31, 719–733.
Tong, L., Tabarrok, B., Wang, T.K., 1992. Simple solution for buckling of orthotropic conical shells. J. Solids Struct. 29, 933–946.
Touloukian, Y.S., 1967. Thermophysical Properties of High Temperature Solid Materials. McMillan, New York.
Woo, J., Mequid, S.A., 2001. Nonlinear analysis of functionally graded plates and shallow shells Int. J. Solids Struct. 38, 7409–7421.
Yang, J., Shen, H.S., 2003. Non-linear analysis of functionally graded plates under transverse and in-plane loads. Int. J. Non-Linear Mech. 38, 467–482.
Zhang, C., Savaids, G., Zhu, H., 2003. Transient dynamic analysis of a cracked functionally graded material by a BIEM. Comput. Mater. Sci. 26, 167–174.